

# 新北市政府 104 年度自行研究報告

研究主題:

中文：

使用電腦輔助分類系統分析肩關節超音波影像以診斷肩旋轉肌病變

英文：

Computer-aided diagnostic system of rotator cuff lesions on shoulder ultrasound images

研究機關：新北市立聯合醫院

研究人員：李忠謙

研究期程：104. 1. 1-104. 12. 31

新北市政府衛生局編印

印製年月：104 年 12 月

# 新北市政府 104 年度自行研究計畫表

填表人：李忠謙

填表日期：103.10.29

聯絡電話：0978695369

計 畫 名 稱	使用電腦輔助分類系統分析肩關節超音波影像以診斷肩旋轉肌病變		
研究機關及人員	計畫主持人：新北市立聯合醫院 骨科 李忠謙主任	期 程	自 104 年 1 月 1 日 至 104 年 12 月 31 日
目 的	發展肩關節電腦輔助分類系統來診斷肩旋轉肌病變及斷裂。		
方 法	藉由分析解剖學上的資訊，將邊緣偵測自動化，準確地區隔出不同組織分層，接著便是發展超音波影像上的紋路特徵於待分析的肩旋轉肌組織，以紋路特徵進行量化分析，最後是紋路特徵超音波影像紋路特徵的量化資料根據，建構電腦輔助分類系統來協助診斷肩旋轉肌疾病。		
經 費	397,000 元		
備 註			

備註：

- 一、研究機關及人員：包括研究機關、實際研究人員及參與工作人員。
- 二、方法：如研究方法之訂定、問題之發掘、研究設計、資料之蒐集與分析、解決方案之研擬、研究報告之提出。
- 三、已提報之自行研究計畫因故撤銷辦理者，應敘明原因行文通知。
- 四、自行研究報告內容應力求與所屬局處業務相關。

## 新北市政府 104 年度自行研究成果摘要表

計 畫 名 稱	使用電腦輔助分類系統分析肩關節超音波影像以診斷肩旋轉肌病變
期 程	自 104 年 1 月 1 日至 104 年 12 月 31 日
經 費	397,000 元
緣 起 與 目 的	發展肩關節電腦輔助分類系統來診斷肩旋轉肌病變及斷裂。
方 法 與 過 程	藉由分析解剖學上的資訊，將邊緣偵測自動化，準確地區隔出不同組織分層，接著便是發展超音波影像上的紋路特徵於待分析的肩旋轉肌組織，以紋路特徵進行量化分析，最後是紋路特徵超音波影像紋路特徵的量化資料根據，建構電腦輔助分類系統來協助診斷肩旋轉肌疾病。
研 究 發 現 及 建 議	The proposed CAD achieved an accuracy of 87.9% for diagnosis of rotator cuff lesions. The individual accuracy of this CAD system was 88.4% for inflammation, 83.3% for calcific tendinitis, and 92.3% for tear groups, respectively.
備 註	

# 新北市政府 104 年度自行研究計畫執行情形季報表

填表日期：

計畫名稱	研究機關及人員	期程		執行情形概述	備註
		起	訖		
使用電腦輔助分類系統分析肩關節超音波影像以診斷肩旋轉肌病變	新北市立聯合醫院骨科 李忠謙主任	104.01.01	104.12.31	1.持續文獻搜尋中。 2.預計參加5月國際研討會。	
使用電腦輔助分類系統分析肩關節超音波影像以診斷肩旋轉肌病變	新北市立聯合醫院骨科 李忠謙主任	104.01.01	104.12.31	1.已完成103年度及104上半年度個案醫學影像收集。 2.電腦輔助分類系統對103年度前之個案做分析已有初步結果。 3.順利發表兩篇國際會議海報論文。(APKASS 2015 Taipei, CARS 2015 Barcelona)	
使用電腦輔助分類系統分析肩關節超音波影像以診斷肩旋轉肌病變	新北市立聯合醫院骨科 李忠謙主任	104.01.01	104.12.31	1.初步成果目前正在撰寫學術論文，已完成introduction及部份material and methos。 2.目前進行不同廠牌之超音波影像之MIP normalization，以期本計畫研發之CADx未來的應用範圍更廣泛。 3.IRB進度:送審中。	
使用電腦輔助分類系統分析肩關節超音波影像以診斷肩旋轉肌病變	新北市立聯合醫院骨科 李忠謙主任	104.01.01	104.12.31	已完成論文寫作，完成AJE論文修改後，將進行國際期刊投稿。	

## **Abstract**

The lifetime prevalence of shoulder pain is up to 70% which is mostly attributed to rotator cuff lesions such as inflammation, calcific tendinitis, and tears. On clinical examination, shoulder ultrasound has been recommended to detect lesions. In this study, a computer-aided diagnosis (CAD) system was developed to reduce the inter-operator variabilities of ultrasound examination for the improvement of practicality. The collected cases included 43 inflammations, 30 calcific tendonitis, and 26 tears. For each case, region size and texture features were extracted from the whole lesion area and combined in a multinomial logistic regression classifier for lesion classification. As a result, the proposed CAD achieved an accuracy of 87.9%. The individual accuracy of this CAD system was 88.4% for inflammation, 83.3% for calcific tendinitis, and 92.3% for tear groups, respectively. The k value of Cohen's Kappa was 0.798. Upon the diagnostic performance, the CAD can provide promising suggestion in clinic use.

**Keywords:** Rotator cuff lesions, should ultrasound, computer-aided diagnosis, texture

## **Introduction**

The prevalence of shoulder pain is high in many countries, and a lifetime prevalence of shoulder pain is up to 70% (Luime et al. 2004), only behind low back pain prevalence (84%) (Walker 2000). In America, shoulder pain costs the health care system 7 billion per year and is the cause of 13% of sick leaves (Hidalgo-Lozano et al. 2010). With respect to the etiologies, up to 70% of shoulder pain is attributed to rotator cuff lesions (Macfarlane et al. 1998; Mitchell et al. 2005). According to Neer's classification system, the lesions of rotator cuff can be classified into inflammation, calcific tendinitis, and full or partial thickness tears. Patients with rotator cuff lesions have shoulder pain, positive impingement sign, limited forward elevation, weak abduction, and external rotation which may induce the difficulties of holding things. Rotator cuff tears with the overall prevalence rate of 20.7% is the most severe type which would cause severe shoulder pain and impingement sign, limited forward elevation and weak abduction and external rotation. Especially for current population with more and more aging people, the prevalence rate of rotator cuff tears would be expected to become higher.

In the treatment of rotator cuff tendinopathy, the status of rotator cuff integrity is deterministic to decide surgical intervention or conservative treatment. Clinical symptoms and physical examination are considered unreliable to diagnose rotator cuff

lesions (Park et al. 2005) because the severity of the rotator cuff tendinopathy affects the diagnostic values of commonly used clinical tests. Additionally, considerable inter-observer variabilities exist between physicians (Beaudreuil et al. 2009). Consequently, clinical assessment relies on imaging modalities to evaluate the integrity of rotator cuff tendons (Murphy et al. 2013). Shoulder X-ray, ultrasound, magnetic resonance imaging and more specific arthrography are available imaging techniques on clinical examination (Shahabpour et al. 2008). Previous literatures recommend shoulder ultrasound as a useful imaging tool to detect rotator cuff lesions (Allen and Wilson 2001; Middleton et al. 2004; de Jesus et al. 2009) and full-thickness rotator cuff tears when performed by experienced musculoskeletal radiologists or shoulder orthopedic surgeon (Smith et al. 2011). The accuracy of ultrasound is comparable with that of magnetic resonance imaging (MRI) (Teefey et al. 2004; de Jesus et al. 2009). To identify partial-thickness rotator cuff tears and other intra-substance tendon abnormalities, the diagnostic performance based on ultrasound is likely reduced under the examinations of general radiologist and ultrasonographers (Smith et al. 2011). To strengthen the clinical use of ultrasound, the inter-operator variabilities should be further reduced.

Computer-aided diagnosis (CAD) system has been proposed to distinguish between benign and malignant lesions such as breast and prostate cancer (Joo et al.

2004; Doi 2005; Giger et al. 2008; Moon et al. 2012a). The advantages of CAD systems are quantitative, efficiency, and consistent. After extracting the quantitative features from lesion area, the complementary abilities of various features are combined in an artificial intelligence classifier to estimate the likelihood being a specific type of lesion. With the assistance of the CAD, the diagnostic performance of seven radiologists in distinguishing between benign and malignant breast lesions were improved (Kashikura et al. 2013). Based on the success of the CAD systems in interpreting ultrasound images, a CAD system based on shoulder ultrasound was proposed in this study to classify rotator cuff lesions such as inflammation, calcific tendinitis, and thickness tears. Numerous region and texture features were implemented in the experiment to diagnose rotator cuff lesions. To the best of our knowledge, this is the first study exploring the performance of quantitative features extracted from the whole rotator cuff lesions in shoulder ultrasound for lesion classification. The result would be especially helpful to assist junior physicians in distinguishing lesions with similar properties on clinical examination.

## **Materials and Methods**

### **Patients and data acquisition**

The institution review board approval was obtained and informed consent was

waived for this retrospective study. The database used in this study consisted of 99 shoulder ultrasound images in 93 adult patients collected from January 2011 to February 2014. The 93 cases were those of 43 men and 50 women aged 31-89 years (mean age, 57.5 years).

The shoulder ultrasound images in the collected database were generated using an ALOKA alpha-6 ultrasound scanner (Hitachi-Aloka Medical, Tokyo, Japan) with linear array probe (scan width: 36mm) ranging from 5 to 13 MHz. The settings of the ultrasound scanner such as gain compensation were consistent for all patients. During examination, the postures of the examined patients were standard sitting position and were followed by the regular routine. After acquisition, the shoulder ultrasound images were drawn out from the scanner and stored as 8-bit images with pixel value ranging from 0 to 255. The lesion types can be classified into three categories including 43 cases of tendon inflammation, 30 cases of calcific tendonitis, and 26 cases of supraspinatus tear. The diagnosis was performed by the consensus of one shoulder orthopaedic surgeon and one physical medicine and rehabilitation physician and was used to evaluate the performance of the proposed CAD system.

### **Contour delineation**

For every image, the lesion contour was manually delineated by a shoulder

orthopaedic surgeon using ImageJ, a medical image processing program developed at the NIH by Wayne Rasband (<http://rsb.info.nih.gov/ij/>). The principle of the delineation procedure was enclosing the lesion area while avoiding normal tendons included. Fig. 1 shows the acquired ultrasound images and the delineation of lesion contour based on the sonographic appearance.

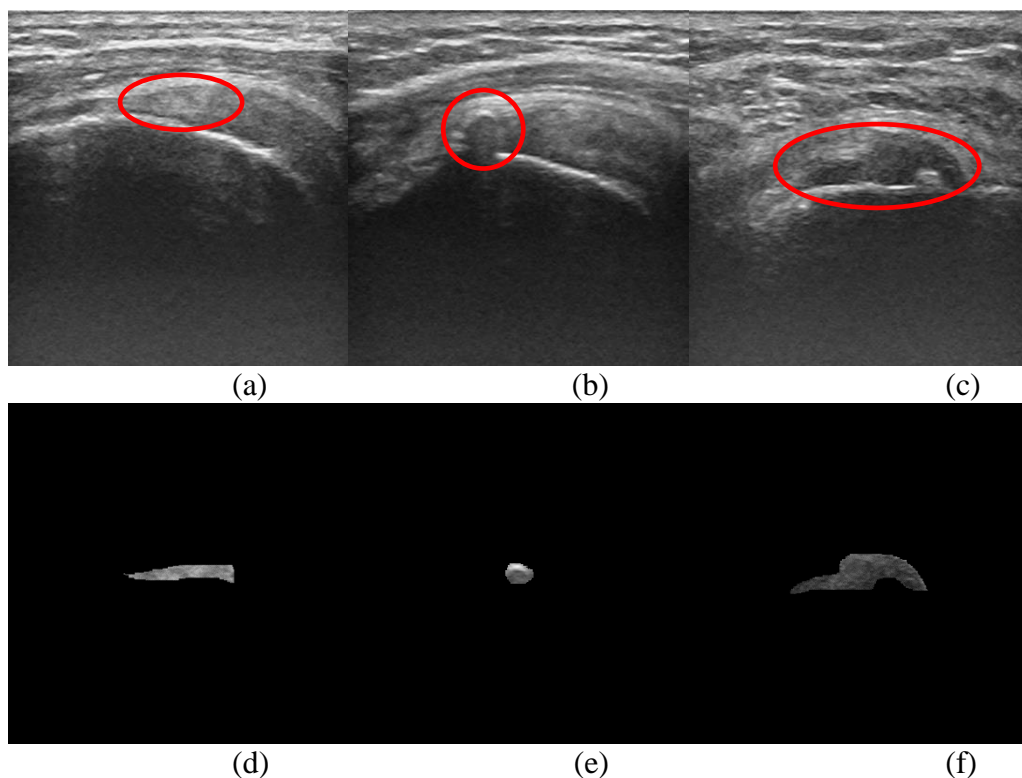


Fig. 1 Various lesions in supraspinatus tendon shown in long-axis ultrasound images. (a) A case of tendon inflammation. (b) A case of calcific tendonitis. (c) A case of supraspinatus tear. (d), (e), (f) The lesion contours of (a), (b), (c) respectively, which were delineated by a shoulder orthopaedic surgeon using ImageJ.

### Feature extraction

Upon the sonographic appearance, the lesion contours which enclosed the specific tissues were obtained after the contour delineation. From the lesion areas, the

region size and texture features were extracted to express tissue characteristics. The normal supraspinatus tendon is a convex beak-shaped hyperechoic structure in long-axis view (Petranova et al. 2012). The features of supraspinatus tendinitis are thickened, irregular, heteroechoic and loss of homogeneous texture with no signs of tears. Calcific tendinitis comes in several forms, and foci of hyperechoic micro-calcification without acoustic shadow is the common form. However, large foci of calcification may be soft or hard and may be solitary or lobulated (Beggs 2011). Soft calcification is fragmented and hyperechoic with well-defined margin and with or without acoustic shadows. Hard calcification has a hyperechoic convex superficial contour often with acoustic shadows (Beggs 2011). On ultrasound, supraspinatus tear appears as hypoechoic areas with irregular margins (Kurol et al. 1991; Allen and Wilson 2001; Vlychou et al. 2009). They could extend from the bursal to the articular surface as the full-thickness tears or affect only a part of tendon thickness as the partial-thickness tears (Beggs 2011).

According to the tissue characteristics mentioned in prior studies, the morphology features widely used in CAD systems may not be useful in lesion classification because there is no certain rule for a specific lesion type. Nevertheless, the region sizes of lesions are the basic properties which can be combined with other features for classification. In the experiment, the number of pixels included in the

delineated lesion area was counted to be the feature of region size.

To quantify the echogenicities of different lesion types, the second-order statistics of ultrasound texture (Moon et al. 2012b) were proposed in this study as quantitative texture features. The second-order statistics describes the correlations between adjacent pixels in the lesion area. In ultrasound images, texture patterns were the combinations of tissue echogenicities expressed by gray-scale. Consequently, analysing the gray-scale co-occurrence matrices (GLCM) (Haralick et al. 1973) representing the correlations between adjacent pixels were proposed to reveal the texture difference between various lesion types.

In GLCM, an image can be quantized to be  $G$  with reduced number of intensity bins,  $N_g$  ( $N_g=64$  in the experiment). Afterward, the  $N_g \times N_g$  co-occurrence matrices  $P=[p(i,j|d,\theta)]$  were generated from  $G$  by scanning each image pixel and its neighbor pixels. The element  $P=[p(i,j|d,\theta)]$  means the frequencies of two neighbor pixel values separated by distance  $d$  and the direction angle  $\theta$ , one has a gray value  $i$  and the other has a gray value  $j$ . Fig. 2 shows the two parameters  $d=1$  and  $\theta=0^\circ, 45^\circ, 90^\circ, 135^\circ$ , used in the GLCM method for the relations among neighboring pixels in the experiment. Four co-occurrence matrices with different angles were considered to extract GLCM features.

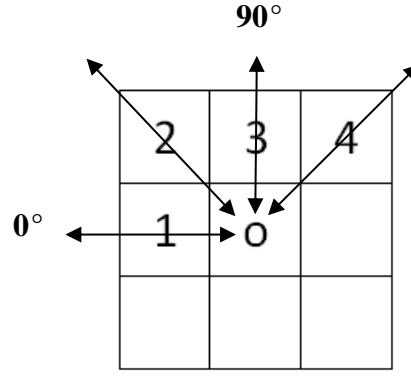


Fig. 2. The pixel pairs of four directions from the centered pixel (o). Pixel 1 to 4 are the neighboring pixels in the direction of 0°, 45°, 90°, and 135° with  $d=1$ , respectively.

Eight GLCM texture features are calculated based on the following formulas:

Energy: 
$$f_1 = \sum_i \sum_j p(i, j|d, \theta)^2 \quad (1)$$

Entropy: 
$$f_2 = -\sum_i \sum_j p(i, j|d, \theta) \log(p(i, j|d, \theta)) \quad (2)$$

Correlation: 
$$f_3 = \frac{\sum_i \sum_j (i - \mu_x)(j - \mu_y) p(i, j|d, \theta)}{\sigma_x \sigma_y} \quad (3)$$

Local Homogeneity: 
$$f_4 = \sum_i \sum_j \frac{1}{1 + (i - j)^2} p(i, j|d, \theta) \quad (4)$$

Inertia: 
$$f_5 = \sum_i \sum_j (i - j)^2 p(i, j|d, \theta) \quad (5)$$

Cluster Shade: 
$$f_6 = \sum_i \sum_j (i + j - \mu_x - \mu_y)^3 p(i, j|d, \theta) \quad (6)$$

Cluster Prominence: 
$$f_7 = \sum_i \sum_j (i + j - \mu_x - \mu_y)^4 p(i, j|d, \theta) \quad (7)$$

Haralick's Correlation: 
$$f_8 = \frac{\sum_i \sum_j (i \cdot j) p(i, j|d, \theta) - \mu_x \mu_y}{\sigma_x \sigma_y} \quad (8)$$

where  $\mu_x, \mu_y, \sigma_x$  and  $\sigma_y$  are mean and standard deviation (SD) of the marginal

distributions of  $p(i, j|d, \theta)$

$$\mu_x = \sum_i i \sum_j p(i, j|d, \theta), \mu_y = \sum_j j \sum_i p(i, j|d, \theta) \quad (9)$$

$$\sigma_x^2 = \sum_i (i - \mu_x)^2 \sum_j p(i, j|d, \theta), \sigma_y^2 = \sum_j (j - \mu_y)^2 \sum_i p(i, j|d, \theta) \quad (10)$$

Consequently, the quantitative texture features including the mean and SD of *Energy*, *Entropy*, *Correlation*, *Local Homogeneity*, *Inertia*, *Cluster Shade*, *Cluster Prominence*, and *Haralick's Correlation* were used to present lesion characteristics such as brightness, relative contrast, and heterogeneity for lesion classification.

### **Statistical analysis**

For lesion classification, all the proposed features were combined in a multinomial logistic regression classifier (Hosmer et al. 2000) to establish a prediction model. Stepwise backward elimination was used to explore the most relevant combination of the subset features. While the least error rate was achieved, the corresponding subset features were selected for the prediction model. The leave-one-out cross-validation (Hosmer et al. 2000) was then used to evaluate the established model regarding the generalization ability. In each iteration, one case was picked from the  $K$  collected cases and was used to test the trained model by the remaining  $K-1$  cases.

Taking the diagnosis determined by agreement of a shoulder orthopaedic surgeon

and one physical medicine and rehabilitation physician as the gold standard, the classification performance of the prediction model was obtained by probabilities. For each case, the likelihoods being inflammation, calcific tendinitis, and tears were generated and were expressed as probabilities. The highest probability value determined the lesion type a case belonging to in the prediction model. Summarizing the cases which were correctly classified, the accuracy was obtained. The test methods used in the experiment were performed by SPSS software (version 16 for Windows; SPSS, Chicago, IL, USA).

The measurement of interrater reliability was performed to examine the agreement of lesion types between the proposed CAD system and the surgeon. As a statistical measure, Cohen's Kappa (Landis and Koch 1977), which ranges from -1.0 to 1.0 where large numbers indicate better reliability, was used to determine how well the implementation of CAD in the experiment. The agreement was considered slight if the  $k$  value was 0.20; fair, if  $k$  between 0.21 to 0.40; moderate, if  $k$  between 0.41 to 0.60; substantial, if  $k$  between 0.61 to 0.80; and almost perfect, if  $k$  between 0.81 to 1.00.

## **Results**

After feature selection, the relevant texture features were selected and combined in the classifier to generate a prediction model. The selected features included Local

Homogeneity (SD), Cluster Shade (mean), Cluster Prominence (mean), Cluster Prominence (SD), and Haralick's Correlation (mean). The performance of the model is listed Table 1. The CAD system achieved an overall accuracy of 87.9%. The individual accuracy of this CAD system was 88.4% for inflammation, 83.3% for calcific tendinitis, and 92.3% for tear groups, respectively.

With respect to the measurement of interrater reliability between the proposed CAD system and the agreement of two interpreters, the resulting k value of Cohen's Kappa was 0.798 which is substantial and statistically significant ( $p < 0.001$ ).

## **Discussion**

A CAD system based on region features and statistical textures was established to interpret tissue echogenicities of shoulder musculoskeletal ultrasound. For distinguishing lesion types, a prediction model built by logistic regression classifier was generated and evaluated. The performance achieved overall accuracy of 87.9% to classify rotator cuff inflammation, calcific tendinitis and tears. The individual accuracy of inflammation and tear groups was relatively higher (88.4% and 92.3%, respectively) and that of calcific tendinitis group was relatively lower (83.3%).

Additionally, the Cohen's Kappa=0.798 which was acquired from the analysis of interrater reliability between the CAD system and the surgeon demonstrates a substantial and statistically significant result ( $p < 0.001$ ).

Previous study (Horng and Chen 2009) which used only a part of lesion tissues (fixed 30×60 pixels) for tissue characterization obtained the accuracy of 92.5%. Based on the accuracies reported in the previous study and this study, texture features are evaluated to be useful in classifying rotator cuff lesions. Nevertheless, extracting quantitative features from the whole lesion area which is proposed in this study is expected to provide more reliable accuracy than the previous study. In the observation of tissue composition, heterogeneity is commonly presented. Using an arbitrary part of lesion to extract lesion features would be too subjective with operator dependence. The variabilities existed between different lesions and observers are considerable.

Ultrasound is a useful diagnostic tool for shoulder disorders and almost as an initial imaging study for detecting rotator cuff lesions. The advantages of ultrasound to detect shoulder lesions have been documented as being quick, relatively cheap, easy to assess and with few contraindications.(Beggs 2006) Most publications of shoulder ultrasound studies demonstrate the sensitivity and specificity of rotator cuff tears. The accuracy of shoulder ultrasound to detect partial and full rotator cuff tears has demonstrated a sensitivity of 46% to 95% and a specificity of 50% to 97% (Mack et al. 1985; Brandt et al. 1989; Soble et al. 1989; Kurol et al. 1991; Wiener and Seitz 1993; van Holsbeeck et al. 1995; Alasaarela et al. 1998; Read and Perko 1998; Teefey et al. 2000; Roberts et al. 2001; Miller et al. 2008). According to the literature reviews, the

inter-observer agreement of rotator cuff lesions from shoulder ultrasound is only poor to moderate due to different operator professions (Kamwendo et al. 1991; de Winter et al. 1999; O'Connor et al. 2005) which implies that additional diagnostic tools like CAD is needed.

The accuracy of proposed CAD in calcific tendinitis group was relatively lower (83.3%). Clinically, calcific tendinitis is found as hyperechoic spots or masses in ultrasound. It is believed that ultrasound has a high diagnostic accuracy for calcific tendinitis although few studies were focused on diagnostic accuracy of calcific tendinitis.(Martin-Hervas et al. 2001; Kayser et al. 2005) Nevertheless, the CAD system did not perform comparably to general radiologist as expected. A possible reason may be the heterogeneity of tissues composing calcific tendinitis. The brightness variabilities existed in different ultrasound settings during image acquisition could affect the texture values. The effect would be stronger for heterogeneity tissues. In the future experiment, intensity-invariant texture features can be developed to reduce the effect caused by brightness variabilities.

Reviewing the literatures, sensitivity and specificity for assessment of full thickness rotator cuff tears are better than that for partial-thickness rotator cuff tears(Middleton et al. 2004; Teefey et al. 2004; Smith et al. 2011). The use of ultrasound for the assessment of partial-thickness rotator cuff tears appeared controversial

(Martin-Hervas et al. 2001; Mitchell et al. 2005; Moosmayer et al. 2007) that is a kind of uncertain issue clinically. In this study, the CAD system achieved high accuracy (92.3%) in tear group including partial or full-thickness tears (Fig. 4) by means of the analysis of tissues enclosed in lesion contour. The performance achieved by quantitative echogenicity texture analysis can provide a clinical suggestion for general radiologist or ultrasonographers who may not achieve accuracy as high as shoulder orthopaedic surgeon (Smith et al. 2011).

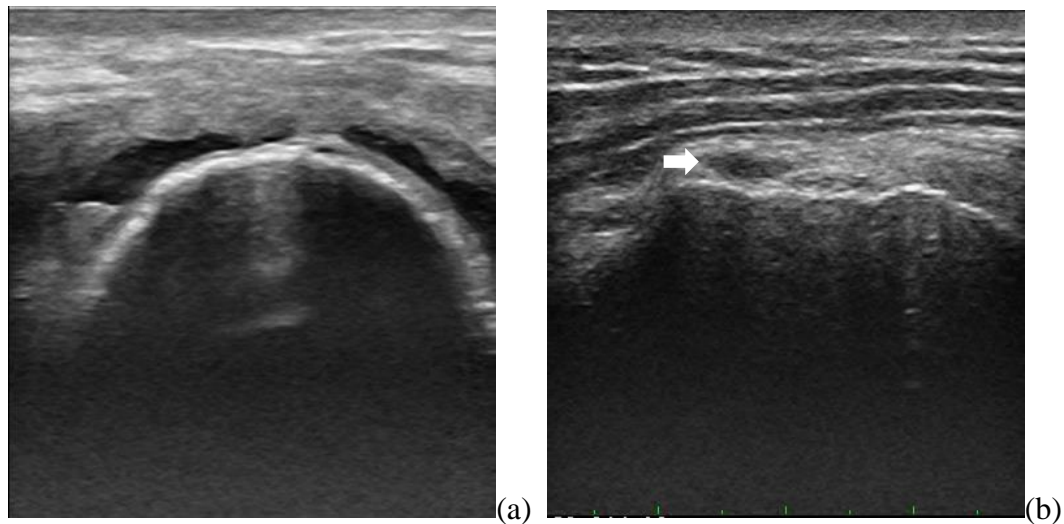


Fig. 4 An example showing the difference between a full-thickness and a partial-thickness supraspinatus tear. (a) A full-thickness supraspinatus tear shows the hypoechoic area, which extends from the bursal to the articular surface. (b) A case of partial-thickness tear shows the focal hypoechoic area (white arrow), which affects only a part of tendon thickness.

More experiments will be accomplished in the future to explore the clinical application of the proposed CAD such as the improvements of different readers' interpretations with CAD. In conclusion, the CAD system based on region features

and statistical textures extracted from the shoulder ultrasound images achieved good accuracy in classifying rotator cuff inflammation, calcific tendinitis and tears. The diagnostic suggestion generated by the proposed CAD would be practical and promising in clinic use.

## **Acknowledgements**

The authors would like to thank the New Taipei City Hospital (NTCH104-001) of Taiwan, the Republic of China for financially supporting this research.

## References

- Alasaarela E, Leppilahti J, Hakala M. Ultrasound and operative evaluation of arthritic shoulder joints. *Annals of the rheumatic diseases* 1998;57:357-60.
- Allen GM, Wilson DJ. Ultrasound of the shoulder. *European journal of ultrasound : official journal of the European Federation of Societies for Ultrasound in Medicine and Biology* 2001;14:3-9.
- Beaudreuil J, Nizard R, Thomas T, Peyre M, Liotard JP, Boileau P, Marc T, Dromard C, Steyer E, Bardin T, Orcel P, Walch G. Contribution of clinical tests to the diagnosis of rotator cuff disease: a systematic literature review. *Joint, bone, spine : revue du rhumatisme* 2009;76:15-9.
- Beggs I. Ultrasound of the shoulder and elbow. *The Orthopedic clinics of North America* 2006;37:277-85, v.
- Brandt TD, Cardone BW, Grant TH, Post M, Weiss CA. Rotator cuff sonography: a reassessment. *Radiology* 1989;173:323-7.
- de Jesus JO, Parker L, Frangos AJ, Nazarian LN. Accuracy of MRI, MR arthrography, and ultrasound in the diagnosis of rotator cuff tears: a meta-analysis. *AJR American journal of roentgenology* 2009;192:1701-7.
- de Winter AF, Jans MP, Scholten RJ, Deville W, van Schaardenburg D, Bouter LM. Diagnostic classification of shoulder disorders: interobserver agreement and

determinants of disagreement. *Annals of the rheumatic diseases* 1999;58:272-7.

Doi K. Current status and future potential of computer-aided diagnosis in medical imaging. *The British journal of radiology* 2005;78 Spec No 1:S3-S19.

Giger ML, Chan HP, Boone J. Anniversary paper: History and status of CAD and quantitative image analysis: the role of Medical Physics and AAPM. *Med Phys* 2008;35:5799-820.

Haralick RM, Shanmugam K, Dinstein IH. Textural features for image classification. *Systems, Man and Cybernetics, IEEE Transactions on* 1973;610-21.

Hidalgo-Lozano A, Fernandez-de-las-Penas C, Alonso-Blanco C, Ge HY, Arendt-Nielsen L, Arroyo-Morales M. Muscle trigger points and pressure pain hyperalgesia in the shoulder muscles in patients with unilateral shoulder impingement: a blinded, controlled study. *Experimental brain research* 2010;202:915-25.

Hong M-H, Chen S-M. Multi-class classification of ultrasonic supraspinatus images based on radial basis function neural network. *J Med Biol Eng* 2009;29:242-50.

Hosmer DW, Lemeshow S, Cook E. *Applied logistic regression* 2nd edition. NY: John Wiley & Sons 2000;

Joo S, Yang YS, Moon WK, Kim HC. Computer-aided diagnosis of solid breast nodules: use of an artificial neural network based on multiple sonographic

features. *IEEE transactions on medical imaging* 2004;23:1292-300.

Kamwendo K, Linton SJ, Moritz U. Neck and shoulder disorders in medical secretaries. Part I. Pain prevalence and risk factors. *Scandinavian journal of rehabilitation medicine* 1991;23:127-33.

Kashikura Y, Nakayama R, Hizukuri A, Noro A, Nohara Y, Nakamura T, Ito M, Kimura H, Yamashita M, Hanamura N, Ogawa T. Improved differential diagnosis of breast masses on ultrasonographic images with a computer-aided diagnosis scheme for determining histological classifications. *Academic radiology* 2013;20:471-7.

Kayser R, Hampf S, Pankow M, Seeber E, Heyde CE. [Validity of ultrasound examinations of disorders of the shoulder joint]. *Ultraschall in der Medizin* 2005;26:291-8.

Kurol M, Rahme H, Hilding S. Sonography for diagnosis of rotator cuff tear. Comparison with observations at surgery in 58 shoulders. *Acta orthopaedica Scandinavica* 1991;62:465-7.

Landis JR, Koch GG. The measurement of observer agreement for categorical data. *biometrics* 1977;159-74.

Luime JJ, Koes BW, Hendriksen IJ, Burdorf A, Verhagen AP, Miedema HS, Verhaar JA. Prevalence and incidence of shoulder pain in the general population; a

systematic review. Scandinavian journal of rheumatology 2004;33:73-81.

Macfarlane GJ, Hunt IM, Silman AJ. Predictors of chronic shoulder pain: a population based prospective study. The Journal of rheumatology 1998;25:1612-5.

Mack LA, Matsen FA, 3rd, Kilcoyne RF, Davies PK, Sickler ME. US evaluation of the rotator cuff. Radiology 1985;157:205-9.

Martin-Hervas C, Romero J, Navas-Acien A, Reboiras JJ, Munuera L. Ultrasonographic and magnetic resonance images of rotator cuff lesions compared with arthroscopy or open surgery findings. Journal of shoulder and elbow surgery / American Shoulder and Elbow Surgeons [et al] 2001;10:410-5.

Middleton WD, Teefey SA, Yamaguchi K. Sonography of the rotator cuff: analysis of interobserver variability. AJR American journal of roentgenology 2004;183:1465-8.

Miller D, Frost A, Hall A, Barton C, Bhoora I, Kathuria V. A 'one-stop clinic' for the diagnosis and management of rotator cuff pathology: Getting the right diagnosis first time. International journal of clinical practice 2008;62:750-3.

Mitchell C, Adebajo A, Hay E, Carr A. Shoulder pain: diagnosis and management in primary care. Bmj 2005;331:1124-8.

Moon WK, Lo CM, Chang JM, Huang CS, Chen JH, Chang RF. Computer-aided classification of breast masses using speckle features of automated breast

ultrasound images. *Med Phys* 2012a;39:6465-73.

Moon WK, Lo CM, Huang CS, Chen JH, Chang RF. Computer-aided diagnosis based on speckle patterns in ultrasound images. *Ultrasound Med Biol* 2012b;38:1251-61.

Moosmayer S, Heir S, Smith HJ. Sonography of the rotator cuff in painful shoulders performed without knowledge of clinical information: results from 58 sonographic examinations with surgical correlation. *Journal of clinical ultrasound : JCU* 2007;35:20-6.

Murphy RJ, Daines MT, Carr AJ, Rees JL. An independent learning method for orthopaedic surgeons performing shoulder ultrasound to identify full-thickness tears of the rotator cuff. *The Journal of bone and joint surgery American volume* 2013;95:266-72.

O'Connor PJ, Rankine J, Gibbon WW, Richardson A, Winter F, Miller JH. Interobserver variation in sonography of the painful shoulder. *Journal of clinical ultrasound : JCU* 2005;33:53-6.

Park HB, Yokota A, Gill HS, El Rassi G, McFarland EG. Diagnostic accuracy of clinical tests for the different degrees of subacromial impingement syndrome. *The Journal of bone and joint surgery American volume* 2005;87:1446-55.

Petranova T, Vlad V, Porta F, Radunovic G, Micu MC, Nestorova R, Iagnocco A.

Ultrasound of the shoulder. *Med Ultrason* 2012;14:133-40.

Read JW, Perko M. Shoulder ultrasound: diagnostic accuracy for impingement syndrome, rotator cuff tear, and biceps tendon pathology. *Journal of shoulder and elbow surgery / American Shoulder and Elbow Surgeons* [et al] 1998;7:264-71.

Roberts CS, Walker JA, 2nd, Seligson D. Diagnostic capabilities of shoulder ultrasonography in the detection of complete and partial rotator cuff tears. *American journal of orthopedics* 2001;30:159-62.

Shahabpour M, Kichouh M, Laridon E, Gielen JL, De Mey J. The effectiveness of diagnostic imaging methods for the assessment of soft tissue and articular disorders of the shoulder and elbow. *European journal of radiology* 2008;65:194-200.

Smith TO, Back T, Toms AP, Hing CB. Diagnostic accuracy of ultrasound for rotator cuff tears in adults: a systematic review and meta-analysis. *Clinical radiology* 2011;66:1036-48.

Soble MG, Kaye AD, Guay RC. Rotator cuff tear: clinical experience with sonographic detection. *Radiology* 1989;173:319-21.

Teefey SA, Hasan SA, Middleton WD, Patel M, Wright RW, Yamaguchi K. Ultrasonography of the rotator cuff. A comparison of ultrasonographic and arthroscopic findings in one hundred consecutive cases. *The Journal of bone and*

joint surgery American volume 2000;82:498-504.

Teefey SA, Rubin DA, Middleton WD, Hildebolt CF, Leibold RA, Yamaguchi K.

Detection and quantification of rotator cuff tears. Comparison of ultrasonographic, magnetic resonance imaging, and arthroscopic findings in seventy-one consecutive cases. The Journal of bone and joint surgery American volume 2004;86-A:708-16.

van Holsbeeck MT, Kolowich PA, Eyler WR, Craig JG, Shirazi KK, Habra GK,

Vanderschueren GM, Bouffard JA. US depiction of partial-thickness tear of the rotator cuff. Radiology 1995;197:443-6.

Vlychou M, Dailiana Z, Fotiadou A, Papanagiotou M, Fezoulidis IV, Malizos K.

Symptomatic partial rotator cuff tears: diagnostic performance of ultrasound and magnetic resonance imaging with surgical correlation. Acta radiologica 2009;50:101-5.

Walker BF. The prevalence of low back pain: a systematic review of the literature

from 1966 to 1998. Journal of spinal disorders 2000;13:205-17.

Wiener SN, Seitz WH, Jr. Sonography of the shoulder in patients with tears of the

rotator cuff: accuracy and value for selecting surgical options. AJR American journal of roentgenology 1993;160:103-7; discussion 9-10.

Table 1 The accuracy of the proposed CAD in classifying rotator cuff lesions.

Group	Pathology	Accuracy
I	Inflammation	88.4%
II	Calcific tendinitis	83.3%
III	Tears	92.3%
Overall		87.9%